*16th World Conference on Earthquake, 16WCEE 2017*

*Santiago Chile, January 9th to 13th 2017*

*Paper N° 903*

*Registration Code: S-D1463062547*

# DYNAMIC RESPONSE OF AN ELASTIC SDOF SYSTEM FIXED ON TOP OF A ROCKING PODIUM FRAME STRUCTURE: MODELLING

J. A. Bachmann[(1)], M. F. Vassiliou[(2)], B. Stojadinović[(3)]

[(1)] *PhD Candidate, Chair of Structural Dynamics and Earthquake Engineering, IBK, ETH Zürich, bachmann@ibk.baug.ethz.ch*
[(2)] *Post-Doctoral Researcher, Chair of Structural Dynamics and Earthquake Engineering, IBK, ETH Zürich, vassiliou@ibk.baug.ethz.ch*
[(3)] *Professor, Chair of Structural Dynamics and Earthquake Engineering, IBK, ETH Zürich, stojadinovic@ibk.baug.ethz.ch*

## *Abstract*

The response of rigid freely rocking SDOF systems has been extensively studied. It has been shown that single large rocking bodies, or single-story frames made of rocking columns capped with a beam of significant weight, are more stable than their smaller, or lighter counterparts under analytical pulse and recorded ground motion excitations. Under such excitations, the lateral forces carried by the rocking body, or the single-story rocking frame, are controlled at the uplift force level and depend on the slenderness of the rocking elements. Furthermore, the excitation energy transmitted to the rocking system is dissipated at every impact, with the frame having no residual displacement at the end of its rocking motion.

Such dynamic response characteristics make freely rocking systems very desirable for their superior seismic performance, but very challenging to design. An analytical model developed to facilitate seismic design of structures supported by a single-story rocking podium frame is presented in this paper. This model comprises an elastic single-degree-of-freedom system fixed to a rigid beam that is rocking on rigid columns. As such, the model is an extension of a previously developed model for a rocking podium frame. This model was used to develop rocking uplift and overturning response spectra for the podium frame structural system under analytical pulse support excitations.

*Keywords: Rocking, Uplift, Seismic Isolation, Podium Structure.*

## 1. Introduction

Seismic base isolation has been used for decades. It decreases the design forces for the isolated superstructure and takes most of the displacement demand through a soft and specially designed layer between the structure and the foundation. Usually this soft layer comprises either rubber or (concave) sliding bearings. Simplified models, experimental validation of them, and code provisions have resulted in increasing use of seismic base isolation.

Another method of seismic isolation has been used in Russia and the former Soviet Union states. The soft layer does not comprise bearings placed under the base slab, but the entire bottom story is intentionally designed as "soft" (but with large displacement capacity). The concrete columns of this story are designed to uplift and sustain rocking motion during an earthquake. Thus, the design forces in the superstructure are controlled by the uplift force of the bottom story. The critical design parameters for such podium building structure are the geometric properties of the columns. Column ends are protected by steel plates to avoid concrete crushing when they uplift. Unlike concave or lead-rubber bearings (which develop hysteretic damping that results in residual displacements), energy dissipation due to uplift and rocking is instantaneous and happens at every impact. Therefore, the rocking podium system has minimal (if any) residual deformation and has a resilient behavior. Added dampers can be used to diminish the magnitude of the rocking motion. Interestingly, full-scale dynamic tests of rocking podium structures have been performed on real structures (Fig. 1). The structures were excited using a hydraulic jack to push the structure to an initial displacement and then release it [1]. It should be mentioned that this system does not rely on the size of the rocking elements for its stability, as the rocking isolation techniques proposed for solitary columns or rocking assemblies do [2–30].

The force-displacement response of concave friction-pendulum and lead-rubber bearings can be approximated by a bilinear envelope curve with positive stiffnesses. This allows for a rough approximation of the base isolated structure response using a secant stiffness linear model with viscous damping [31, 32]. On the contrary, a rocking podium structure has negative post-uplift stiffness (the restoring force decreases as the lateral displacement increases). It has been proven that these kinds of structural systems cannot be approximated by a SDOF elastic systems and, hence, the widely used elastic response spectra are not applicable [5].

This paper presents a simplified model to describe the behavior of an elastic structure sitting on a rocking podium. The model was validated using the results from small-scale experiments performed in the Institute of Structural Engineering (IBK) of the Swiss Federal Institute of Technology (ETH) in Zurich [33].


Fig. 1 – Full-scale dynamic tests of a rocking podium structure [1]

## 2. Proposed Analytical Rocking Model

The proposed model is an extension of the model presented in [16, 20]: An elastic SDOF system is added on top of a rigid rocking frame. Fig. 2 shows the model in its initial and uplifted (rocking) position. In order for it to represent rocking podium buildings, it is assumed that the dynamic response of the superstructure can be adequately described using an elastic SDOF. The elastic superstructure is assumed to have no distributed mass along its height and the top mass is assumed to be concentrated. Since the columns are identical with the same dimensions and a rotational inertia $I_c$ around their center of mass, the rigid cap beam (with mass $m_b$) translates in its plane without rotation.

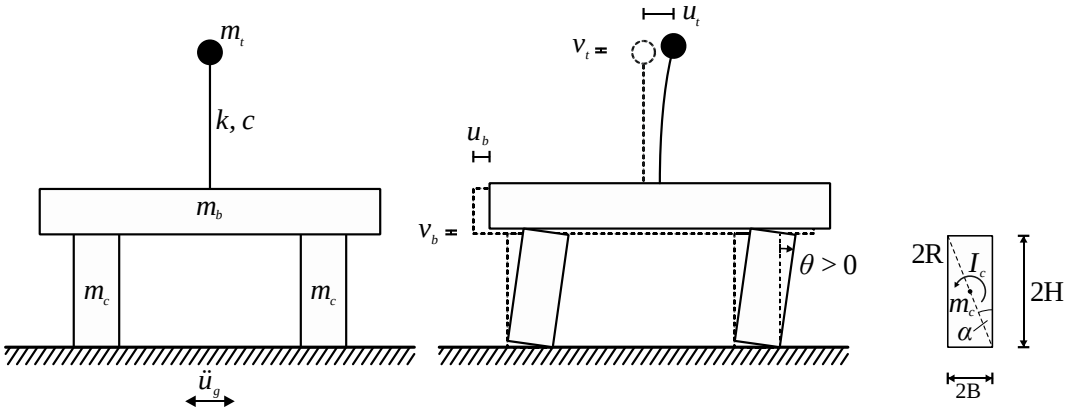


Fig. 2 – Dynamic model of a rocking podium structure.
Left: Initial position. Middle: Rocking position. Right: Dimensions of a column

The slenderness $\alpha$ of the column governs the rocking behavior of the podium structure. It is defined as:

$$\tan\alpha = \frac{2B}{2H} = \frac{B}{H} \tag{1}$$

where 2$B$ is the width and 2$H$ the height of one column. Evidently, assuming that the columns of the rocking frame are adequately protecting against corner crushing, the displacement capacity of the first floor is equal to 2B.

The mass ratios $\gamma$ (for the cap beam) and $\eta$ (for the superstructure), and a rotational inertia factor $\lambda$ are introduced:

$$\gamma = \frac{m_b}{2m_c}, \quad \eta = \frac{m_t}{2m_c} \tag{2}$$

$$\lambda = \frac{I_c}{m_c R^2} \tag{3}$$

where $\lambda$ depends on the shape, size R and mass distribution of the columns. For a rigid block with an evenly distributed mass $m_c$ the factor $\lambda$ is 1/3.

### 2.1 Equation of Motion Before Uplift and Uplift Criterion

The SDOF system representing the structure on the rocking podium has a fixed-base natural frequency $\omega_s$ and a viscous damping ratio $\zeta$. Before uplift of the rocking frame, its equation of motion is:

$$\ddot{u}_t + 2\zeta\omega_s\dot{u}_t + \omega_s^2 u_t = -\ddot{u}_g \tag{4}$$

A single column [2] and an array of $N$ free-standing columns capped with a rigid beam [16] uplift when:

$$\left|\ddot{u}_g\right| > g\tan(\alpha) \tag{5}$$

In the model presented herein, the deformability of the superstructure changes the uplift criterion.

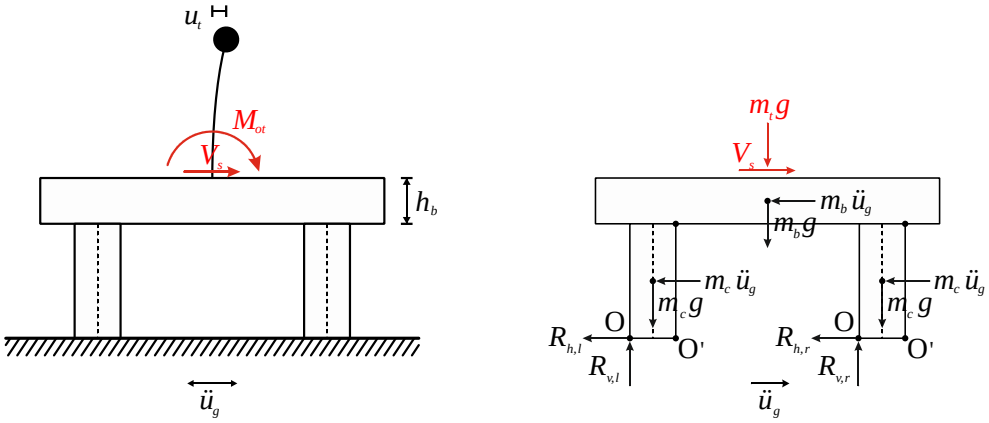


Fig. 3 – Left: Overturning moment and story shear of the superstructure. Right: Forces at incipient uplift.

Fig. 3 (right) shows the forces acting on the columns at incipient uplift (for $\theta < 0$). Applying the principle of virtual work for a positive $\ddot{u}_g$ and a resulting virtual rotation of $-\delta\theta$ at this instant yields:

$$2\cdot\delta\theta\left(Bm_c g - Hm_c\ddot{u}_g\right) + \delta\theta\cdot 2B\left(m_b g + m_c g\right) - \delta\theta\cdot 2Hm_b\ddot{u}_g + \delta\theta\cdot 2HV_s = 0 \tag{6}$$

$$V_s = m_t\left(\omega_s^2 u_t + 2\zeta\omega_s\dot{u}_t\right) \tag{7}$$

It is assumed that the rigid cap beam is heavy enough such that the overturning base moment of the SDOF superstructure cannot separate it from the supporting columns. Combining Eq. (6) and Eq. (7) yields:

$$\ddot{u}_g\left(m_c + m_b\right) = g\tan(\alpha)\left(m_c + m_b + m_t\right) + \omega_s^2 m_t u_t + 2\zeta\omega_s m_t\dot{u}_t \tag{8}$$

With Eq. (2) the uplift thresholds for both positive and negative ground accelerations are:

$$\ddot{u}_g = \pm\left[g\tan(\alpha)\frac{1+2\gamma+2\eta}{1+2\gamma}\right] + \left(\omega_s^2 u_t + 2\zeta\omega_s\dot{u}_t\right)\frac{2\eta}{1+2\gamma} \tag{9}$$

For top light superstructures ($\eta << \gamma$) the ground acceleration limit given by Eq. (9) will converge to the values given by Eq. (5).

## 2.2 Equations of Motion After Uplift

Lagrangian formulation is used to derive the equations of motion after uplift:

$$\frac{d}{dt}\frac{\partial L}{\partial \dot{q}_i} - \frac{\partial L}{\partial q_i} = Q_{q_r}$$
$$L = T - V \tag{10}$$

where $T$ is the kinetic energy stored in the system and $V$ the potential energy defined by Eq. (11). $Q_{qr}$ is the generalized form for a conservative force, derived from virtual work $W$ done in the system for a displacement $\delta q_r$.

$$V = -\int \vec{F} \cdot d\vec{r} \tag{11}$$

$$Q_{q_r} = \frac{\delta W}{\delta q_r} \tag{12}$$

To simplify the computation, vertical and horizontal translations of the rigid cap beam, both depending solely on column rotation angle $\theta$ (Fig. 2), are introduced:

$$\begin{aligned} u_b &= 2R\left(\pm\sin\alpha - \sin\left(\pm\alpha - \theta\right)\right) \\ v_b &= 2R\left(\cos(\pm\alpha - \theta) - \cos\alpha\right) \end{aligned} \tag{13}$$

The first and second derivatives with respect to time of Eq. (13) are:

$$\begin{aligned} \dot{u}_b &= 2R\dot{\theta}\cos(\pm\alpha - \theta) \\ \ddot{u}_b &= 2R\left[\ddot{\theta}\cos(\pm\alpha - \theta) + \dot{\theta}^2\sin(\pm\alpha - \theta)\right] \end{aligned} \tag{14}$$

$$\begin{aligned} \dot{v}_b &= 2R\dot{\theta}\sin(\pm\alpha - \theta) \\ \ddot{v}_b &= 2R\left[\ddot{\theta}\sin(\pm\alpha - \theta) - \dot{\theta}^2\cos(\pm\alpha - \theta)\right] \end{aligned} \tag{15}$$

The top mass displacement is captured as a total displacement with components $u_t$ and $v_t$ where $v_t$ is assumed to be equal to the cap beam displacement $v_b$. The kinetic energy in the system is:

$$T = T_t + T_b + T_c = \frac{1}{2}m_t\left(\dot{u}_t^2 + \dot{v}_t^2\right) + \frac{1}{2}m_b\left(2R\dot{\theta}\right)^2 + 2\frac{1}{2}m_c\left(R\dot{\theta}\right)^2 + 2\frac{1}{2}I_c\dot{\theta}^2 \tag{16}$$

where $I_c$ is the rotational inertia around the center of mass of a single column. Eq. (16) can be simplified, considering that

$$\dot{v}_t = \dot{v}_b \tag{17}$$

holds, to:

$$T = \frac{1}{2}m_t\left(\dot{u}_t^2 + 4R^2\sin^2(\pm\alpha - \theta)\dot{\theta}^2\right) + \frac{1}{2}m_b\left(2R\dot{\theta}\right)^2 + 2\frac{1}{2}m_c\left(R\dot{\theta}\right)^2 + 2\frac{1}{2}\lambda m_c\left(R\dot{\theta}\right)^2 \tag{18}$$

The potential energy in the system is:

$$V = 2Rg\left(m_t + m_b + 2\frac{1}{2}m_c\right)\cos\left(\pm\alpha - \theta\right) + \frac{1}{2}m_t\omega_s^2\left(u_t - u_b\right)^2 + m_t\ddot{u}_g u_t - 2R\ddot{u}_g\left(m_b + 2\frac{1}{2}m_c\right)\sin\left(\pm\alpha - \theta\right) \tag{19}$$

To account for damping in the system, the virtual work performed by a viscous damper positioned between the cap beam and the mass of the superstructure is:

$$\delta W = f_D \cdot \delta q_r = -c\left(\dot{u}_t - \dot{u}_b\right)\cdot\left(\delta u_t - \delta u_b\right) = -2\zeta m_t\omega_s\left(\dot{u}_t - \dot{u}_b\right)\cdot\left(\delta u_t - 2R\cos\left(\pm\alpha - \theta\right)\delta\theta\right) \tag{20}$$

where $u_b$ and its time derivative are defined by Eq. (13) and Eq. (14), respectively. Applying Eq. (10) to the superstructure mass degree of freedom, $u_t$, yields:

$$m_t\ddot{u}_t + m_t\omega_s^2\left(u_t - u_b\right) + m_t\ddot{u}_g = -2\zeta m_t\omega_s\left(\dot{u}_t - \dot{u}_b\right) \tag{21}$$

Reformulation leads to the first of the two equations of motion:

$$\ddot{u}_t + 2\zeta\omega_s\left(\dot{u}_t - 2R\dot{\theta}\cos(\pm\alpha - \theta)\right) + \omega_s^2\left(u_t - 2R\left(\pm\sin\alpha - \sin\left(\pm\alpha - \theta\right)\right)\right) = -\ddot{u}_g \tag{22}$$

The similarity to Eq. (4) is obvious.

The equation of motion for the other degree of freedom, $\theta$, can be determined similarly. Namely:

$$\begin{aligned} &m_b 4R^2\ddot{\theta} + m_c 2R^2\ddot{\theta}(1+\lambda) + m_t 4R^2\left[\ddot{\theta}\sin^2\left(\pm\alpha - \theta\right) - \dot{\theta}^2\cos\left(\pm\alpha - \theta\right)\sin\left(\pm\alpha - \theta\right)\right] \\ &+2Rg\left(m_t + m_b + 2\frac{1}{2}m_c\right)\sin\left(\pm\alpha - \theta\right) + 2R\ddot{u}_g\left(m_b + 2\frac{1}{2}m_c\right)\cos\left(\pm\alpha - \theta\right) \\ &-2Rm_t\omega_s^2\left(u_t - u_b\right)\cos\left(\pm\alpha - \theta\right) - 4R\zeta m_t\omega_s\left(\dot{u}_t - \dot{u}_b\right)\cos\left(\pm\alpha - \theta\right) = 0 \end{aligned} \tag{23}$$

Eq. (23) can be simplified and rewritten as:

$$\begin{aligned} &\ddot{\theta}\left[3\gamma + \frac{3}{4}(1+\lambda) + 3\eta\sin^2\left(\pm\alpha - \theta\right)\right] = 3\eta\left[\dot{\theta}^2\cos\left(\pm\alpha - \theta\right)\sin\left(\pm\alpha - \theta\right)\right] \\ &-p^2\left(2\eta + 2\gamma + 1\right)\sin\left(\pm\alpha - \theta\right) - \frac{\ddot{u}_g}{g}p^2\left(2\gamma + 1\right)\cos\left(\pm\alpha - \theta\right) \\ &+\frac{3\eta\omega_s}{2R}\left[\omega_s\left(u_t - u_b\right)\cos\left(\pm\alpha - \theta\right) + 2\zeta\left(\dot{u}_t - \dot{u}_b\right)\cos\left(\pm\alpha - \theta\right)\right] \end{aligned} \tag{24}$$

where $p$ is a normalized size parameter with units [1/s], defined as:

$$p^2 = \frac{3g}{4R} \tag{25}$$

## 2.3 Impacts

The proposed rocking model dissipates energy through structural damping of the SDOF model of the superstructure and through rocking impacts of the columns. Two equations are needed to treat the impact and the energy dissipated at impact. The model proposed by Housner [2] presumes that impacts are instantaneous and that the contact forces between the rocking column and the surfaces are concentrated at the pivot points.

Therefore, at the moment of impact, the pivot point instantaneously moves from O to O' and vice versa (see Fig. 3). The above assumption leads to Conservation of Angular Momentum (CoAM) of each column during impact. Moreover, it is assumed that the elastic deformation of the superstructure is small compared to its size, so CoAM is applied in the undeformed configuration. Then CoAM yields the first equation needed. The second equation comes from the assumption that the total horizontal velocities of the top mass before and after impact are equal:

$$\dot{u}_{t,after} = \dot{u}_{t,before} \tag{26}$$

The above assumptions yield the following equation for the coefficient of restitution:

$$c = \frac{\dot{\theta}^2_{after}}{\dot{\theta}^2_{before}} = \left[ 1 - \frac{\sin^2(\alpha)\left(2\gamma + 2\eta + \frac{1}{2}\right)}{\frac{1}{4}(1+\lambda) + \gamma + \eta} \right]^2 \tag{27}$$

Eq. (27) can be compared to the expressions for coefficient of restitution of other, simpler, systems. With $\eta = \gamma = 0$ it yields exactly what Housner proposed for his rigid block, and with $\eta = 0$ its solution is equal to the expression of Makris and Vassiliou [16] for an array of free-standing columns capped with a free-standing rigid beam.

## 2.4 Uplifted Frequency

Once the podium is uplifted, the frequency that the superstructure SDOF is oscillating with changes. To compute the uplifted frequency, the eigenfrequency equation

$$\left| K - \omega^2_{s,up} M \right| = 0 \tag{28}$$

is solved. The authors acknowledge that in the presence of damping, the above equation would be formally correct only if damping satisfies the Caughey O'Kelly condition [34], which is not the case. However, since the damping of the superstructure is small, Eq. (28) is expected to give a good approximation of the uplifted frequencies. This was experimentally confirmed for other elastic uplifting systems [27].

First, the equations of motion (Eq. (22) and Eq. (24)) are linearized. Then, the gravity and ground motion loading terms are neglected. The remaining equations of motion can be expressed in matrix form:

$$\begin{bmatrix} 3\gamma + \frac{3}{4}(1+\lambda) + 3\eta\sin^2\alpha & 0 \\ 0 & 1 \end{bmatrix} \begin{pmatrix} \ddot{\theta} \\ \ddot{u}_t \end{pmatrix} + \begin{bmatrix} 3\eta\omega_s^2\cos^2\alpha & -\frac{3\eta\omega_s^2\cos\alpha}{2R} \\ -2R\omega_s^2\cos\alpha & \omega_s^2 \end{bmatrix} \begin{pmatrix} \theta \\ u_t \end{pmatrix} = \begin{pmatrix} 0 \\ 0 \end{pmatrix} \tag{29}$$

Solving the eigenvalue problem for Eq. (29) yields:

$$\omega^4_{s,up}\left(3\gamma + 3\eta\sin^2\alpha + \frac{3}{4}(\lambda+1)\right) - \omega^2_{s,up}\omega^2_s\left(3\gamma + 3\eta + \frac{3}{4}(\lambda+1)\right) = 0 \tag{30}$$

The eigenfrequency analysis reveals the two distinct mode shapes of the podium structure. The first one is overturning of the podium structure with a natural frequency of 0 Hz, a rigid body motion mode. The second one is the vibration of the SDOF system when the podium structure is uplifted. In this state the natural eigenfrequency $\omega_{s,up}$ is amplified compared to its fixed-base counterpart, $\omega_s$, and is given by Eq. (31):

$$\omega_{s,up} = \sqrt{\frac{\lambda + (4\gamma + 4\eta + 1)}{\lambda + (4\gamma + 4\eta \sin^2 \alpha + 1)}} \cdot \omega_s \tag{31}$$

For heavy superstructures ($\eta \to \infty$) the amplification factor simplifies to 1/sin($\alpha$).

### 2.5 Excitation

Analytical pulses were used to excite and analyze the dynamic response of the proposed analytical model of a rocking podium structure and a rocking podium structure specimen tested on the ETH IBK shaking table. Symmetric and antisymmetric Ricker pulses (Fig. 4) were used:

$$\ddot{u}_g = a_p \left(1 - \frac{2\pi^2 t^2}{T_p^2}\right) e^{-\frac{1}{2}\frac{2\pi^2 t^2}{T_p^2}} \qquad \ddot{u}_g = \frac{a_p}{\beta}\left(\frac{4\pi^2 t^2}{3T_p^2} - 3\right)\frac{2\pi t}{\sqrt{3}T_p} e^{-\frac{1}{2}\frac{4\pi^2 t^2}{3T_p^2}} \tag{32}$$

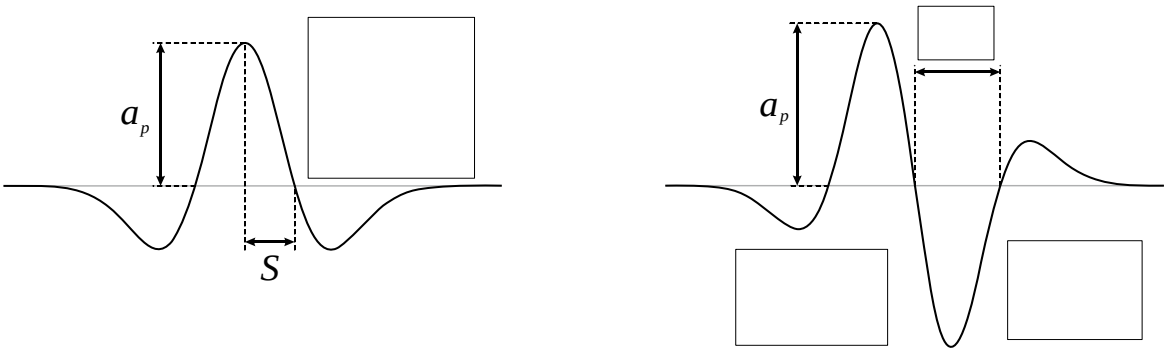


Fig. 4 – Analytical pulses: Left, symmetric Ricker (Mexican hat) pulse; Right, antisymmetric Ricker pulse

## 3. Model Validation Against Test Data

In order to validate the proposed analytical rocking model a specimen shown in Fig. 5 (left) was developed [33]. To the extent possible, the scaled specimen was designed to be physically similar to a prototype rocking podium structure that has realistic properties. Therefore, the specimen beams and cap beam were designed to be as stiff as possible (to approach the rigid columns and cap beam assumption) and as light as possible (the columns of the prototype structure are a small part of its total weight). The superstructure could not be represented by a single mass mounted on a single threaded rod fixed to the rocking podium structure (as was done in [29]), because of the propensity for out of plane motion. Therefore, a frame-like structure with a significant depth was chosen to ensure

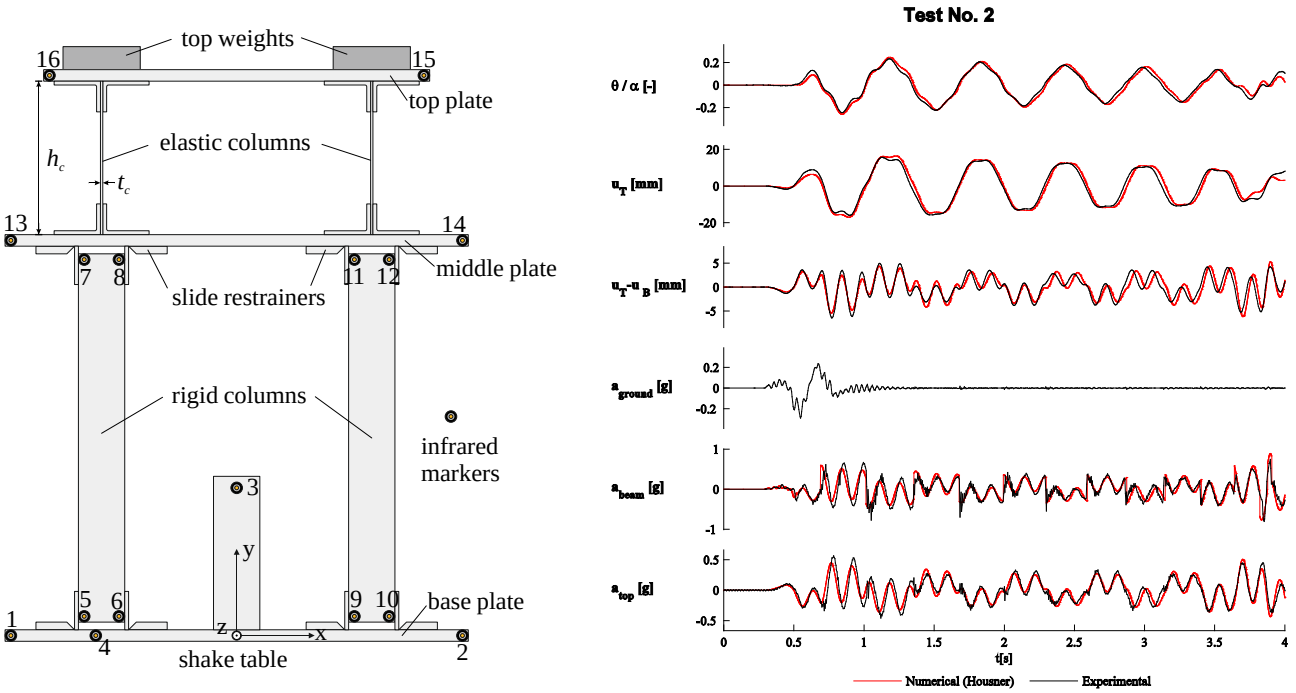


Fig. 5 – Left: Model of a rocking podium structure. Right: Experimental vs. analytical results

that the motion of the SDOF system is restricted to one plane. Similarly, the rocking columns were constrained to move in one plane only.

A realistic structure would have a podium story height of 3m. Due to the laboratory space and test conduct constraints, the specimens was scaled down by a length factor of 6. To preserve acceleration scaling, the excitation ground motions used were scaled in time. For more details on the scaling, an interested reader is referred to [33].

Fig. 5 (right) shows the comparison between the response of the proposed analytical model and the response of the podium structure specimen to an antisymmetric Ricker wavelet with $a_p$ = 0.20g and $T_p$ = 0.30s (at the scaled model scale). At the Prototype scale this value corresponds to a SDOF system period of 0.74s. The analytical model (excited by the applied shaking table excitation signal) matches the recorded response of the specimen quite well.

## 4. Spectra

Fig. 6 plots rocking spectra for the rocking podium structure for different parameter settings. From left to right, the natural period $T_s$ of the superstructure SDOF was increased from 0s (rigid) to 1s (deformable) ($T_s \in$ {0s, 0.1s, 0.5s, 1s}) corresponding to $\omega_s / p$ values of 28.4, 5.7, and 2.8. From top to bottom, the weight of the superstructure, defined by Eq. $(2)_2$, was increased ($\eta \in$ {10, 50, 100}). Assuming that additional floors on top of the rocking one weigh the same, $\eta/\gamma$ can be interpreted as the number of additional floors fixed to the rocking podium structure ($\eta/\gamma \in$ {1, 5, 10}).

The spectra at the bottom ($\eta/\gamma$ = 10) left ($T_s$ = 0s) of Fig. 6 corresponds to the spectra of a rocking rigid frame [16] with $\gamma = 10 \cdot (1+10) = 110$. For a podium story height of 3m the size parameter $p$ (Eq. (25)) is 2.214 Hz. In order to overturn the structure ($\theta/\alpha > 1$) with a symmetric Ricker wavelet with $T_p$ = 1s and $\omega_p$ / p = 2.83 the pulse peak acceleration $a_p$ has to be 3.5 times the uplifting acceleration $\ddot{u}_g$ = 0.15g. For a pulse with a peak acceleration just 2.5 times the uplifting acceleration the maximum rotation of the base column is only 0.29 $\theta/\alpha$. Close to the overturning limit state, the rotation grows fast with increasing $a_p$. The spectra illustrate this superbly with their growing colored areas.

All computed spectra show a similar trend. Overturning only happens for pulses in the long pulse duration range with moderate to high peak ground accelerations. For pulses with periods between 0.7s and 0.95s ($3 < \omega_p / p < 4$) the structures can only be overturned by pulses with peak ground accelerations on the order of 0.9g or more. From a certain point on, here $\omega_p / p > 5$ or $T_p < 0.6$s, it is essentially impossible to overturn the structure by a symmetric Ricker pulse.

Fig. 7 plots the minimum overturning acceleration for the 12 spectra in Fig. 6. In the short period range, the podium structure with a deformable SDOF superstructure is more stable, while in the long period range it becomes less stable than the podium structure with a rigid SDOF superstructure. For a SDOF superstructure with period $T_s = 0.1$s, the system behaves essentially as its rigid counterpart. For longer superstructure periods ($T_s > 0.5$s) the influence of deformability is beneficial for short period pulses and detrimental for long period pulses. The green and blue lines in Fig. 7 indicate this trend. This can be attributed to pre-uplift resonance of the superstructure since $T_p$ is between 0.95s and 1.4s in the region $2 < \omega_p / p < 3$.

The influence of the weight of the superstructure has a smaller effect than its natural period. As Fig. 7 shows, the performance of heavier structures is only marginally better than that of their lighter counterparts. This aligns well with what [16] stated. Increasing $\gamma$ from 10 ($\eta = 0$) to 20 ($\eta = 1$) only slightly improves the performance of the podium structure.

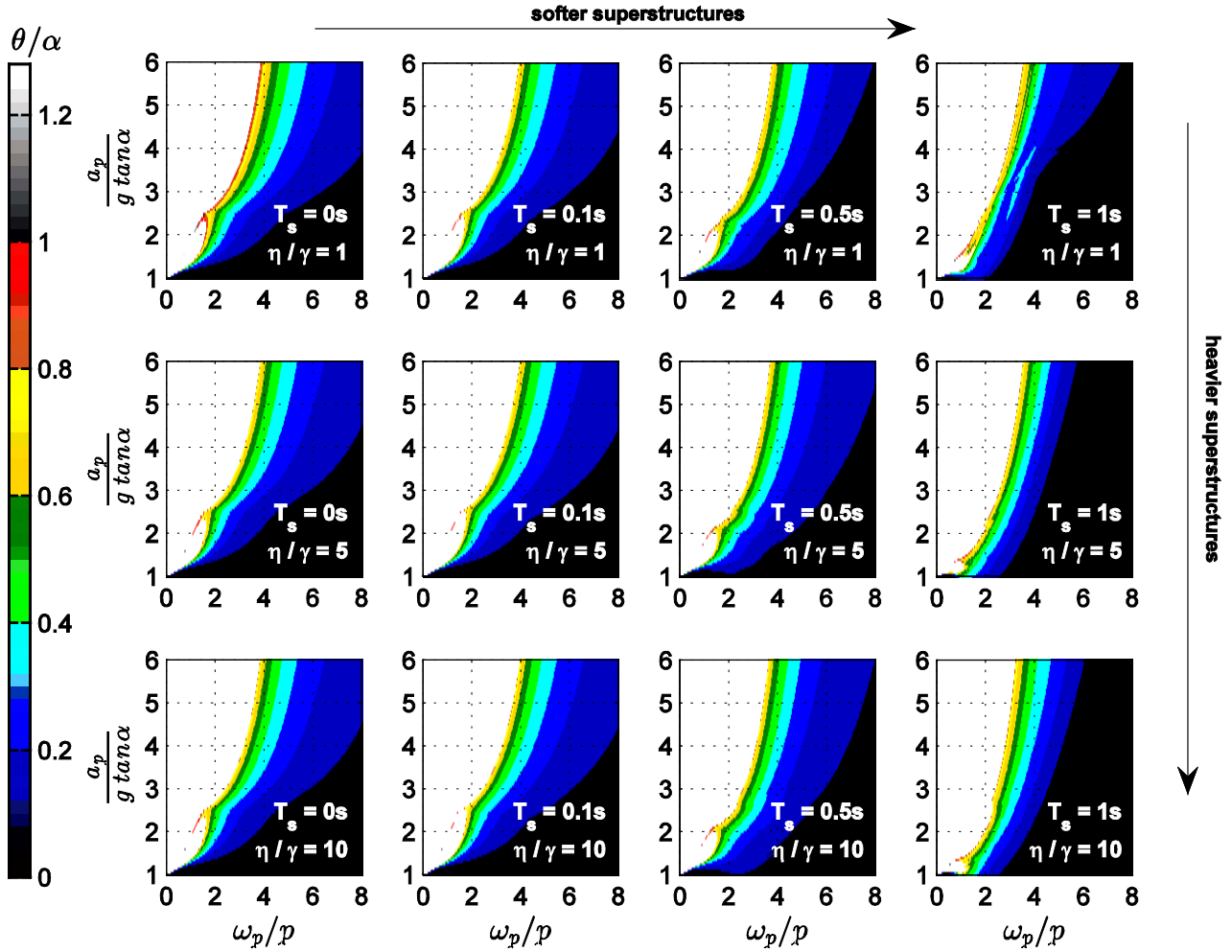


Fig. 6 – Rocking spectra (maximum base rotation, $\theta/\alpha$) of a rocking podium structure with $\gamma = 10$ and different values for $T_s$ (0s, 0.1s, 0.5s, 1s) and $\eta/\gamma$ (1, 5, 10) subjected to a symmetric Ricker wavelet ("Mexican Hat")

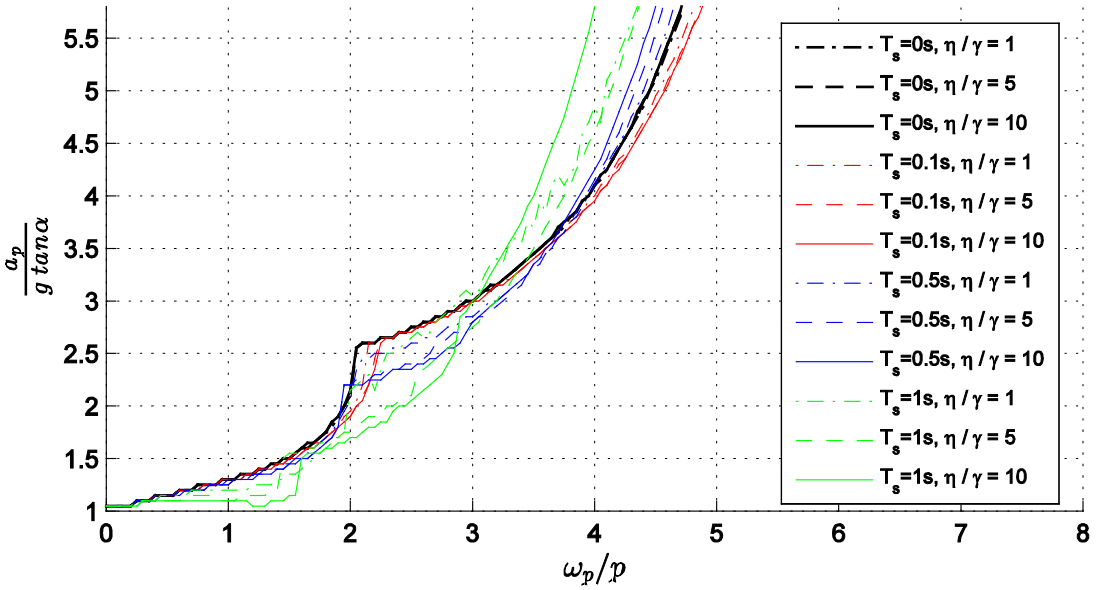


Fig. 7 – Overturning spectra for rocking podium structure subjected to a symmetric Ricker wavelet

## 5. Conclusions

A model to compute the rocking response of rocking podium structure with a deformable cantilever fixed on top of it has been proposed. This model extends the previously developed model [16]. The proposed modified model was verified and validated by comparing the computed response to the response measured in experiments described in the companion paper [33]. The model was then used to construct rocking spectra for rocking podium structures with an elastic oscillator on top exposed to Ricker wavelet ground motion excitations.

Subjected to a symmetric Ricker wavelet, a deformable superstructure with $T_s \geq 0.5$s that is fixed to a rocking podium structure improves the performance of the system in the short period range of the exciting ground motion while it only marginally decreases the stability of the system in the long period range. The weight of the superstructure does not significantly affect the response of the system when the rocking podium structure is heavy compared to the weight of the supporting columns ($\gamma > 10$), which is the case in typical structures.

## 6. References

[1] Семенов С (Semenov S) (2015): Сейсмоизоляция Protection against earthquake. [Online]. Accessed 2016. Available: https://www.youtube.com/watch?v=sZ5KCX2wMd0.

[2] Housner GW (1963): The Behavior of inverted Pendulum Structures during Earthquakes. *Bull. Seismol. Soc. Am.*, **53** (2), 403-417.

[3] Makris N, Roussos Y (1998): Rocking response and overturning of equipment under horizontal pulse-type motion. *Rept. No. PEER Report-98/05*, Pacific Earthquake Engineering Research, Berkeley, USA.

[4] Zhang J, Makris N (2001): Rocking Response of Free-Standing Blocks under Cycloidal Pulses. *J. Eng. Mech.*, **127** (5), 473-483.

[5] Makris N, Konstantinidis D (2003): The rocking spectrum and the limitations of practical design methodologies. *Earthq. Eng. Struct. Dyn.*, **32** (2), 265-289.

[6] Konstantinidis D, Makris N (2005): Seismic response analysis of multidrum classical columns. *Earthq. Eng. Struct. Dyn.*, **34** (10), 1243-1270.

[7] Papaloizou L, Komodromos P (2009): Planar investigation of the seismic response of ancient columns and colonnades with epistyles using a custom-made software. *Soil Dyn. Earthq. Eng.*, **29** (11–12), 1437-1454.

[8] Konstantinidis D, Makris N (2010): Experimental and analytical studies on the response of 1/4-scale models of freestanding laboratory equipment subjected to strong earthquake shaking. *Bull. Earthq. Eng.*, **8** (6), 1457-1477.

[9] Ma QTM (2010): The mechanics of rocking structures subjected to ground motion.

[10] Acikgoz S, DeJong MJ (2012): The interaction of elasticity and rocking in flexible structures allowed to uplift. *Earthq. Eng. Struct. Dyn.*, **41** (11), 1-18.

[11] Dimitrakopoulos EG, DeJong MJ (2012): Revisiting the rocking block: closed-form solutions and similarity laws. *Proc. R. Soc. A Math. Phys. Eng. Sci.*, **468** (2144), 2294-2318.

[12] Dimitrakopoulos EG, DeJong MJ (2012): Overturning of Retrofitted Rocking Structures under Pulse-Type Excitations. *J. Eng. Mech.*, **138** (8), 963-972.

[13] Gelagoti F, Kourkoulis R, Anastasopoulos I, Gazetas G (2012): Rocking isolation of low-rise frame structures founded on isolated footings. *Earthq. Eng. Struct. Dyn.*, **41 (**7), 1177-1197.

[14] Vassiliou MF, Makris N (2012): Analysis of the rocking response of rigid blocks standing free on a seismically isolated base. *Earthq. Eng. Struct. Dyn.*, **41** (2), 177-196.

[15] Dimitrakopoulos EG, DeJong MJ (2013): Seismic overturning of rocking structures with external viscous dampers. *Springer*.

[16] Makris N, Vassiliou MF (2013): Planar rocking response and stability analysis of an array of free-standing columns capped with a freely supported rigid beam. *Earthq. Eng. Struct. Dyn.*, **42** (3), 431-449.

[17] Vassiliou MF, Mackie KR, Stojadinović B (2013): Rocking Response of Slender, Flexible Columns under Pulse Excitation. *COMPDYN 2013*, Greece.

[18] Drosos V; Anastasopoulos I (2014): Shaking table testing of multidrum columns and portals. *Earthq. Eng. Struct. Dyn.*, **43** (11), 1703-1723.

[19] Makris N (2014): The Role of the Rotational Inertia on the Seismic Resistance of Free-Standing Rocking Columns and Articulated Frames. *Bull. Seismol. Soc. Am.*, **104 (**5), 2226-2239.

[20] Makris N, Vassiliou MF (2014): Are Some Top-Heavy Structures More Stable? *J. Struct. Eng.*, **140** (5), 06014001.

[21] Makris N, Vassiliou MF (2015): Dynamics of the Rocking Frame with Vertical Restrainers. *J. Struct. Eng.*, **141** (10), 04014245.

[22] Dimitrakopoulos EG, Giouvanidis AI (2015): Seismic Response Analysis of the Planar Rocking Frame. *J. Eng. Mech.*, **141** (7), 04015003.

[23] Dimitrakopoulos EG, Paraskeva TS (2015): Dimensionless fragility curves for rocking response to near-fault excitations. *Earthq. Eng. Struct. Dyn.*, **44** (12), 2015-2033.

[24] Makris N (2014): A half-century of rocking isolation. *Earthquakes Struct.*, **7** (6), 1187-1221.

[25] Makris N, Vassiliou MF (2015): The dynamics of the rocking frame. *Springer.*

[26] Makris N, Vassiliou MF (2015): Seismic Response and Stability of the Rocking Frame. *Springer*.

[27] Truniger RE, Vassiliou MF, Stojadinović B (2015): An analytical model of a deformable cantilever structure rocking on a rigid surface: experimental validation. *Earthq. Eng. Struct. Dyn.*, **44** (13).

[28] Vassiliou MF, Makris N (2015): Dynamics of the Vertically Restrained Rocking Column. *J. Eng. Mech.*, **141** (12), 04015049.

[29] Vassiliou MF, Truniger RE, Stojadinović B (2015): An analytical model of a deformable cantilever structure rocking on a rigid surface: development and verification. *Earthq. Eng. Struct. Dyn.*, **44** (13).

[30] Makris N, Kampas G (2016): Size Versus Slenderness: Two Competing Parameters in the Seismic Stability of Free - Standing Rocking Columns. *Bull. Seismol. Soc. Am.*, **106** (1), 104-122.

[31] Kelly J (1993): Earthquake-resistant design with rubber. *Springer*.

[32] Makris N, Black CJ (2004): Dimensional Analysis of Bilinear Oscillators under Pulse-Type Excitations. *J. Eng. Mech.*, **130** (9), 1019-1031.

[33] Bachmann JA, Jost C, Studemann Q, Vassiliou MF, Stojadinović B (2016): An analytical model for the dynamic response of an elastic SDOF system fixed on top of a rocking single-story frame structure: experimental validation. *ECCOMAS Congress 2016*, Crete, Greece.

[34] Acikgoz S, DeJong MJ (2016): Analytical modelling of multi-mass flexible rocking structures. *Earthq. Eng. Struct. Dyn.*, **41** (11), 1549-1568.